INVESTIGATION OF THE LOW FLUX SERVO-CONTROLLED LIMIT OF A COPHASED INTERFEROMETER

Luc DAMÉ, Marc DERRIEN, Mathias KOZLOWSKI, Mohamed MERDJANE
Service d'Aéronomie du CNRS, BP 3, 91371 Verrières-le-Buisson Cedex, FRANCE

and

Bertrand CALVEL
MATRA MARCONI SPACE, 31 rue des cosmonautes, 31402 Toulouse Cedex 4, FRANCE

RÉSUMÉ - Dans le cadre du programme spatial SOLARNET (un interféromètre solaire imageur de 3 télescopes de 35 cm de diamètre sur une base circulaire de l'ordre du mètre), nous développons une maquette de laboratoire à 3 petits télescopes cophasés. Sur ce système, représentatif de SOLARNET, nous avons tout particulièrement étudié pour l'ESA (dans le cadre d'un contrat sur la Synthèse d'Ouverture Optique) les limites de stabilité du contrôle des différences de chemin optique (par des lignes à retard à deux étages) quand des objets de référence de plus en plus faibles sont utilisés pour l'asservissement. La méthode de mesure, les hypothèses, les résultats et leur analyse sont présentés qui indiquent aujourd'hui, de manière conservative, qu'un contrôle actif de la phase entre deux télescopes à mieux que $\lambda/100$ peut être obtenu pour des télescopes de l'ordre du mètre avec des étoiles de référence de magnitude 10.

ABSTRACT *- In the framework of the SOLARNET space programme (an imaging solar interferometer of 3 telescopes of 35 cm diameter on a 1 meter circular baseline), we are developing a complete laboratory breadboard of a three-telescopes cophased interferometer. On this representative system we have, in particular, investigated for the European Space Agency (contract on Optical Aperture Synthesis Technology) the limit of the servo-controlled optical path delays (we use active delay lines with 2-stages) when low fluxes reference sources are used. The measurement method, hypothesis and results will be explicated that led to a conservative active control of the phase at 100th of a wavelength for a one-meter class telescope on magnitude 10 stars.*

1 - INTRODUCTION

Service d'Aéronomie is involved since many years in the design and validation of phase control methods aimed at the cophasing — to a fraction of a wavelength — of an optical aperture synthesis system of 3 to 7 telescopes. This experimental program comes in support of the High Resolution Solar Physics Missions (SIMURIS) proposed since 1989 and based on a compact and cophased interferometric configuration at 4 (SUN, the "Solar Ultraviolet Network"), 5 (MUST, the "Multi-mirror Ultraviolet Solar Telescope") and finally 3 telescopes: SOLARNET, the current minimum but optimized design for instantaneous imaging of a large solar field-of-view at high resolution proposed for the CNES Intermediate Missions (PROTEUS Platform) and next ESA Medium Mission (F2/F3). To demonstrated the basic principle of our interferometric imaging approach, the cophasing of two telescopes on extended objects, we built a first laboratory breadboard in 1992 which was able of automatic fringes acquisition and phase stabilization up to $\lambda/300$ (Damé, 1994, Damé et al. 1995, Damé, 1996). In 1995 and 1996 this breadboard was even adapted to observe directly on the sky, the stars, the planets and the Sun, and indeed showed that cophasing on extended objects was not only possible in principle but also in practice (Damé, 1997, Damé et al., 1997).

The results obtained during these years in the various domains covered, both theoretically (generalized coherence modelisation of the fringe pattern) and experimentally (on the successive breadboards), now allow to propose a complete design for a representative demonstrator breadboard of the minimal basic space interferometer - 3 cophased telescopes - and able to perform aperture synthesis imagery. The "real world" imagery test is essential to validate the interactions in this complex system, between reference interferometers, with pointing but also with the fringes/images recording system and the necessary associated noise.

The study presented hereafter on the low flux limit of a cophased interferometer is one step in this demonstration made possible thanks to a contract with Philippe ROUSSEL from the European Space Agency (with MATRA MARCONI SPACE leading the contract) and with the CNRS Service d'Aéronomie in charge for the studies and experiments on Optical Path Difference (OPD) control.

2 - COPHASING AN OPTICAL APERTURE SYNTHESIS SYSTEM: THE DOUBLE SYNCHRONOUS DETECTION TECHNIQUE

Interferometers aim at achieving high resolution by using a set of small telescopes separated by a more or less important distance, rather than a large single telescope. Imaging can be obtained only if the beams from the various telescopes are added in phase in a common focal plane. In the SOLARNET configuration (cf. Fig. 1), the distance between telescopes is small compared to their diameter so that the MTF has no zeros. This is a "compact" system, low dilution one, as opposed to most of the stellar systems where distances between telescopes are large, at least compared to the telescope diameter. Nevertheless, despite this difference, the cophasing technique for both interferometers is the same if high quality (image dynamics) and large field-of-view are expected. The OPD must be controlled to a fraction of a wavelength which means first, a phase measure and, then, the appropriate correction.

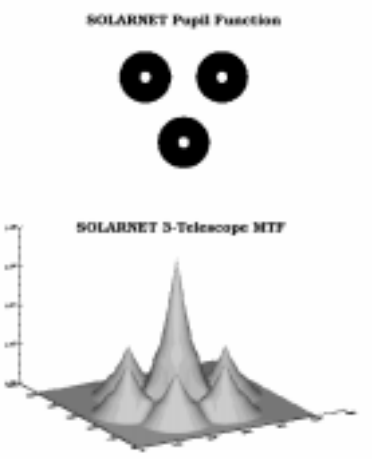

Fig. 1 - SOLARNET configuration (3 x Ø35 cm telescopes on a 1 m baseline) and MTF.

The phase measure is achieved by the use of a synchronous demodulation. The OPD is modulated in one arm of a reference interferometer which makes that the fringes are displaced in time when we are in the coherence zone where the fringes are present. It is worth recalling that the method is an *absolute OPD method* which provides calibrated fringes amplitude by the use — while the fringe position is servo-controlled by the error signal of a first synchronous demodulation — of a second synchronous demodulation at *twice* the reference frequency. This second synchronous detection, at twice the frequency, measures the amplitude of the signal while the first synchronous detection is active. By this mean, and since the first synchonous detection is active (we are stabilized on the submit of the fringe then), the **amplitude of the fringe is directly measured**. By this mean not only we find the fringes (first synchronous detection) but also (and directly) the most prominent one, i.e., normally, the central one at **OPD zero**.

An important aspect of this detection is, then, the contrast of the fringes but also their relative contrast. If we assume a point source (for extended sources, see Damé et al., 1997) and that the light is not monochromatic, from its spectrum we can calculate the mutual coherence function Γ:

$$\Gamma(\mathbf{u_1},\mathbf{u_2},\tau) = \int_0^\infty e^{-2\pi i\nu\tau} d\nu$$

where ν is the frequency and τ the retardation time. The mutual coherence function has the dimensions of intensity. From it can be defined the dimensionless degree of coherence γ:

$$\gamma(\mathbf{u}_1,\mathbf{u}_2,\tau) = \frac{\Gamma(\mathbf{u}_1,\mathbf{u}_2,\tau)}{\sqrt{I(\mathbf{u}_1)\, I(\mathbf{u}_2)}}$$

which is the direct observable quantity of optics, the contrast, being measured by simple interference between two coherent beams of light. In a simple Michelson we have the further advantage of both the *addition* interferogram and the *subtracted* interferogram, with a phase difference of π between the signals (useful in low visibility cases). We have modeled (cf. Fig. 2) both the fringe contrast, the result of a synchronous detection applied to it and of a double (twice the frequency) synchronous detection. As expected, the synchronous detection signal is maximum when we are not on the fringes peaks (and zero on the peaks so that is it a good signal to servo-control on the fringes) but the double synchronous detection is directly proportional to the fringe amplitude and thus provides a direct indicator of the central fringe.

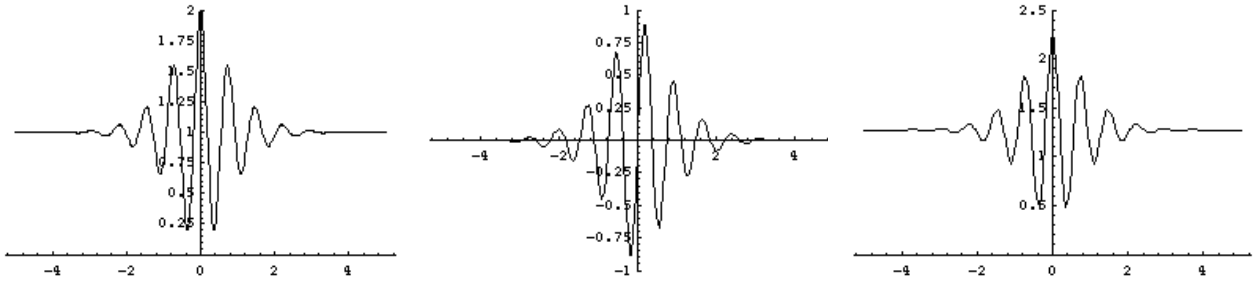

Fig. 2 - Illustration of a fringe signal, its synchronous detection, and the synchronous detection at twice the modulation frequency, as a function of the optical path delay (in μm) for a large "white-light" spectrum ($\Delta\lambda \approx 300$ nm).

3 - PRESENTATION OF THE DEMONSTRATOR

The aim of the demonstrator is to prove that the chosen concept of co-phasing and pointing is, first, compatible with the required imaging performances and, second, outperforming the other possible methods. It must also use techniques which are considered as best candidates for the future larger systems envisaged by ESA. Considering the future trends for space instruments the emphasis has been put on access to the UV part of the spectrum (no fibers) and to the global demonstration of cophasing and pointing on a true imaging system./ This is really a system study of the principle, not yet an engineering model of any kind since, as shown on Fig. 3 and 4, no miniaturization effort has been made. It is evident, for example, that the reference interferometers in a real space instrument will be a handful large (molecular binding) rather than a meter long like in our current laboratory work. Nevertheless the specifications and tolerances of the space system will be directly deduced from the studies on the laboratory breadboard.

A major issue is to qualify the global control that we have on the system and its influence on the imaging potential. A discussion on the control approach can be found in Damé et al. (1997).

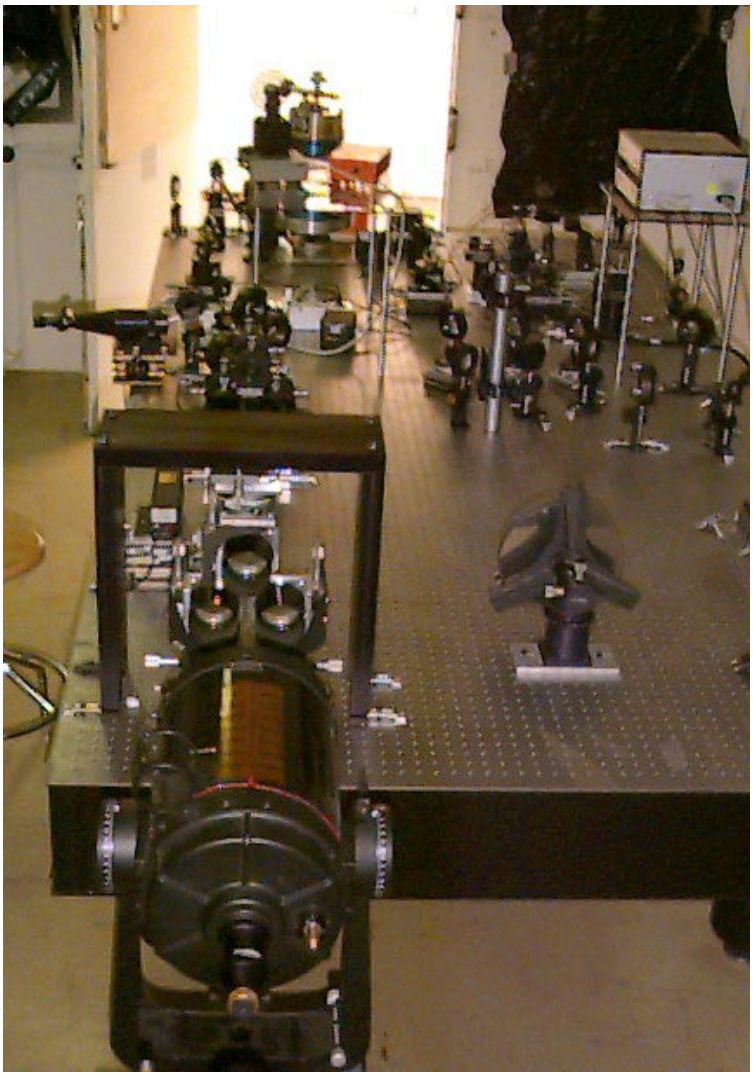

Fig. 3 - Picture of the 3-Telescopes breadboard showing the collimator (Celestron 8) and the 3 refractors (Ø60 mm) which simulates the three telescopes of SOLARNET.

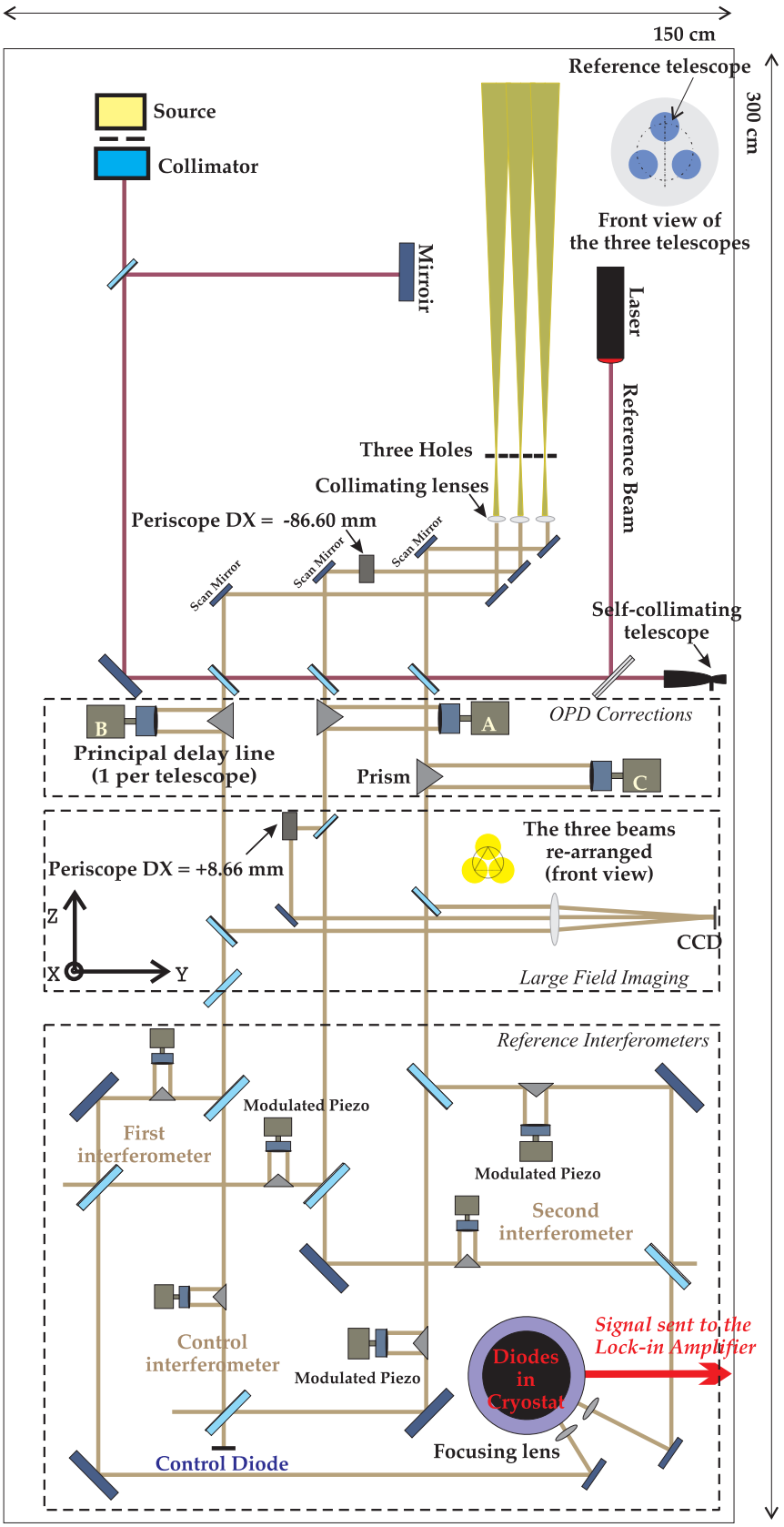

Fig. 4 - Schematic illustration of the new 3 telescopes breadboard under realization for demonstrating all the complex and interacting system aspects of an imaging interferometer (cascading or parallel phase control, pointing influence, CCD dynamics, etc.).

4 - LOW FLUX SIMPLIFIED SETUP

For the low flux study we used only a part of the 3 telescopes breadboard in a simplified setup since only two interfering beams are required. And, because we did not wanted to modified the 3-telescopes setup of the SOLARNET breadboard, we kept the basic components using the reference source and the set of the tree reference plates (simple beam splitters) to feed a two-beams simple interferometer. In order to equalize the path in glass due the beamsplitters, 3 beamsplitters were added, "a", "b" and "c" (cf. Fig. 5).

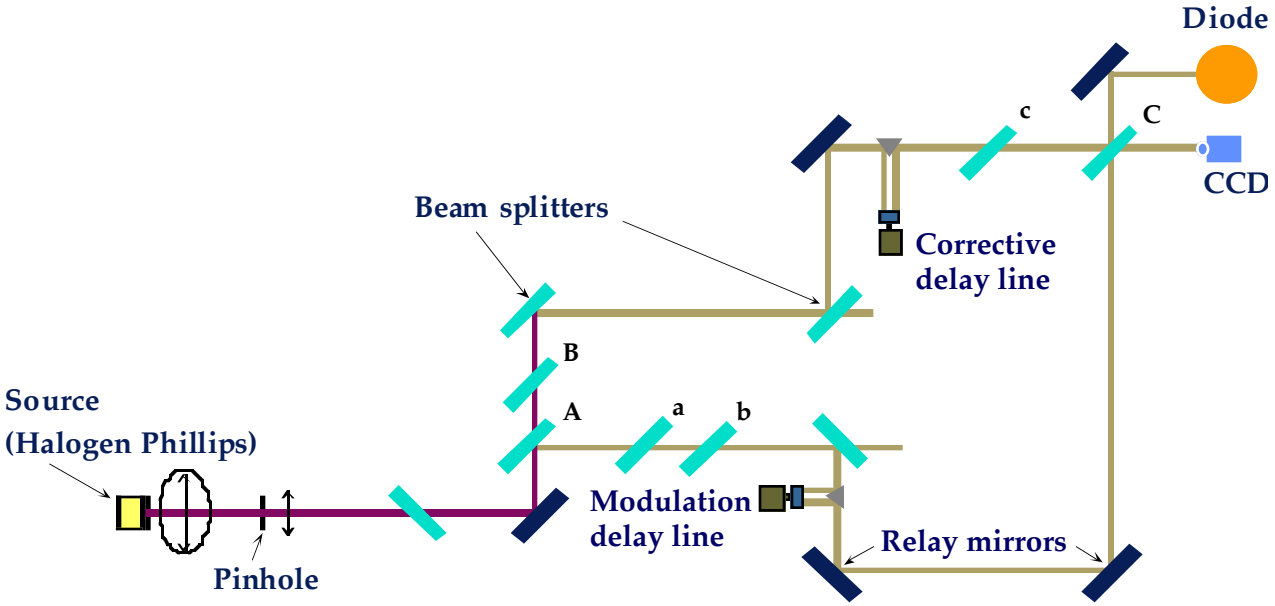

Fig. 5 - Setup used for the low flux study (not to scale). Note the important number of beamsplitters required on each beam in order to equalize the glass transmission to the detector ("a" and "b" compensate for "A" and "B" and "c" for "C", since beamsplitter "C" is of a different thickness than "A" and "B").

With such a setup (6 beamsplitters 50/50 and 4 mirrors!) we indeed start with very low flux since the measured transmission from after the pinhole (10 μm) to just before the diode is only 0.3 ± 0.02% (a 3 for 1000 transmission). This transmission was measured using an absolute photometer (cf. hereafter) and several pinhole sizes (10, 15, 20, 30 and 50 μm) carefully avoiding vignetting.

The beamsplitters are of 2 series (but equally distributed in each arm), either 2.5 or 1.5 mm thick, each with a tolerance of ± 0.1 mm (although probably similar since each serie was made in one time, substrate and evaporation). We considered that this was not a disadvantage for the study since we wanted low fluxes but, as we will see, the dispersion considerations linked to even minor thickness variations can be extremely annoying.

5 - CONTRAST CALIBRATION

5.1 - Photometer and diode

Our objective in this section is to calibrate the contrast that we are measuring. In this process, we are using a photometer (inherited from SPACELAB) to calibrate the flux on the diode independently from its response. The absolute photometer is a model 40 X from United Detector Technology equipped with a radiometric filter for direct absolute measurement in μW. Accordingly, we expect to indicate the flux limit of the system with a maximum error of one stellar visual magnitude (factor 2.5).

A verification of the measurement (order of magnitude at least) made by the photometer is obtained by characterizing the flux received on the diode from its spectral response (using the response curve of the product) and the diode amplifier. The diode is an Hamamatsu S2386-18K (Metal Case) Ø1.1 mm (1.2 mm^2) with an efficiency of ~ 0.45 A/W around 700 nm. It is not a particularly reliable record since the diode is old (8 years or so) and the spectral radiant sensitivity curve a generic one. However, this provides an estimation. The diode amplifier also is several years and was measured back in 1990 to be 20 10^8 V/A.

From this we can calculate the diode response:

$$R_D \approx 0.45 \times 20\ 10^8 = 0.9\ 10^9\ V/W = 0.9\ mV/pW$$

5.2 - Magnitude evaluation

In order to specify a Limit Magnitude we need to make clear several assumptions. The first is that we specify the value as of the visual magnitude outside the atmosphere. In other words, accordingly to Allen (1955):

$$(m_v = 0) \equiv 2.43\ 10^{-10}\ phot = 2.43\ 10^{-6}\ W/m^2$$

The second assumption concerns the Reference System. We assume a *1 m telescope* primary and a central obstruction of 20% (20 cm secondary). This gives a collecting area of *0.754 m^2*. We also assume a *transmission efficiency* to the cophasing system of this reference flux of *10 %*. Accordingly:

$$(m_v = 0) \equiv 2.43\ 10^{-6} \times .754 \times 0.1 \times 2 = 0.366\ \mu W$$

5.3 - System transmission

The absolute photometer measurements are made on the reference flux using a 10 μm pinhole so that the initial flux is already very low. With this system a flux at the level of the source, after the pinhole, is measured to be 0.32 μW. The system transmission, up to the focusing lens on the diode is 0.3 %, as measured using the photometer. The quantum efficiency (QE) of the diode need to be accounted since it is included in our theoretical assumption of the 1 meter telescope with a global transmission of 10% (accounting the QE of the detector). This is more than 70% on the domain 700-1000 nm. We keep 50% to be conservative and also because the diode system is several years old and behind a lens and several windows inside the cryostat (screens).

Reference flux for the 10 μm pinhole with the absolute photometer:

$$0.32\ \mu W \times 0.3\% \times 50\% = 0.00048\ \mu W$$

This is 763 times less than the $m_v = 0$ flux, i.e.:

$$\text{Ref. Magnitude} = \frac{\ln 763}{\ln 2.5} = 7.2$$

A verification that this estimate comes from the direct diode measurement. The diode measures a current of about 200 mV (when modulated using the chopper, i.e. 1/0.6 more without chopping):

$$\sim 200\ mv\ @\ 280\ Hz \Rightarrow 330\ mv,\ \text{i.e. } 0.00037\ \mu W$$

This is only 23 % difference with the absolute measure. This difference is not surprising accounting the assumptions made on the diode sensitivity and transmission from the last beam splitter to the diode and convince us that the precision looked for (one stellar magnitude — a factor 2.5) is certainly achieved. If the diode rather than the absolute photometer was taken as reference for the magnitude calculation (this could be considered since based on the measured current and since the absolute photometer calculation is also affected by the uncertainty on the QE), the Ref. Magnitude would be 7.5.

5.4 - Calibration of the reference contrast

With the pinhole of 10 μm (no vignetting) and using the chopper (@ 280 Hz), the synchronous detection yield 5.5 Vpp. The chopper takes only 60% of the flux into account since the beam size is half the size of the spacing. The true voltage for the full modulation of the signal (100 % contrast) is therefore $5.5 \times 0.6^{-1} = 9.17$ Vpp.

Since we measure a fringe maximum amplitude with synchronous detection (no chopper: directly by scanning the fringe pattern) a mere 2.6 Vpp, this means that our contrast is of only:

$$\text{Ref. Contrast} = \frac{2.6}{9.17} \Rightarrow 28\%$$

6 - RESULTS

To our surprise, the fringe signal was far from containing only a few fringes (5 or so) as in our previous experiments with a white light source and a simple Mach-Zehnder (Damé et al., 1997). It is true that our light source was different (a nice point source of 1 mm diameter opposed to a rather inhomogeneous halogen source) but that could not explain by itself the rather long coherence length and, consequently, numerous fringes observed (cf. Fig. 6). At some point (cf. the two last recording with a neutral optical density of 1.6 - transmission of 2.5%) it was evident that some kind of alignment problem of the blue and red parts of the source spectrum was involved since we could virtually double the fringe pattern (but partly at the expense of the fringe amplitude: lower contrast). The coherence length cannot be explained by the spectrum in output, even though some filtering is made by the cumulative effects of the numerous beamsplitters because it is still around 300 nm (cf. Fig. 9). The next section will bring a beginning of answer to the question.

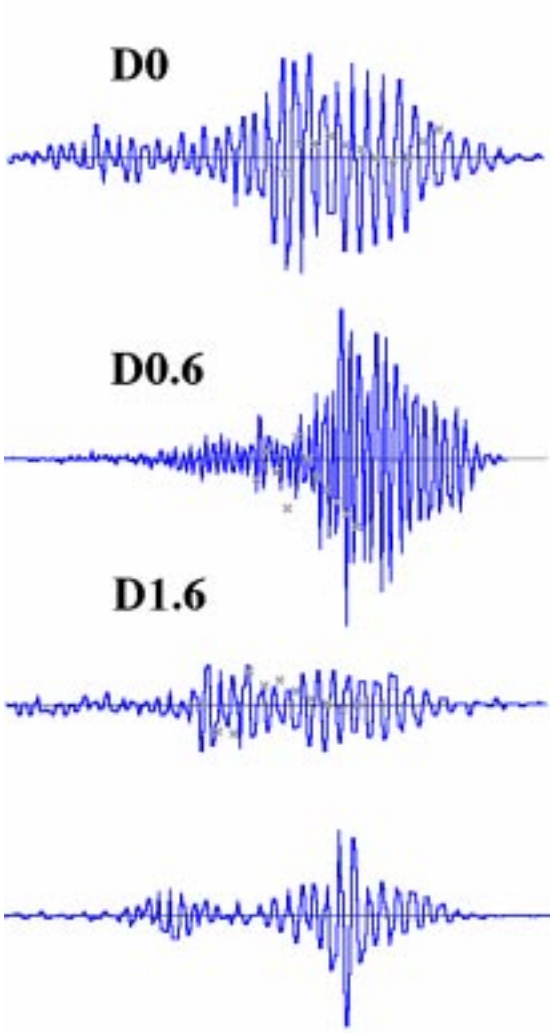

Fig. 6 - Fringe pattern recorded for different optical densities (effect of re-alignment of the beams - beamsplitters orientation in particular - on the last two, D1.6 recordings).

Despite this poor fringe pattern which could limit the measured contrast and, then, stabilities, we performed the low flux study. This was done by adding calibrated neutral density filters (just before the diode) in order to lower the flux progressively. We first defined the value in mV corresponding to an OPD of λ, using a chopper and a slightly variable reference frequency, correcting the measurement for the beam /spacing ratio (Vpp = 9.17 V). Then we find the fringes and locate and measure the larger one using our double synchronous detection method. This gives us the Vpp SD (for Synchronous Detection). On this fringe we servo-control the OPD. The interferometer is large and opened to the air so has to present natural fluctuations up to about 10 Hz (cf. Fig. 7). These are fairly well representative of the constraints expected by ESA for the future space interferometers so that no other mean of introducing defects was considered. Fourier transform of these data (not shown) well indicate that errors/corrections have some power up to 10 Hz. Suppressing the slowly varying component (high pass Butterworth filter at 2 Hz) gives the σ of the residual fluctuations which is used to calculate the stability at 6 σ peak-to-peak (± 3 σ), i.e. a true stability figure and not an RMS one. As shown on Table 1, stabilities achieved are excellent. We reach λ/361 pp on a magnitude 7.2 star and yet a stability of λ/100 on a magnitude 9 star.

Optical density	Flux (nW)	Magnitude (m_v)	Vpp SD (V)	σ fluctuations (mV)	Stability λ/ (pp @ **6σ**)
None	0.48	7.2	2.6	1.2	361.1
0.3	0.24	8.0	3.4	2.7	206.8
0.6	0.12	8.7	3.4	3.8	149.1
1.0	0.048	9.8	1.3	6.6	50.5
1.3	0.024	10.5	3.5	38.5	15.2
1.6	0.012	11.3	1.6	26.1	10.2
2.0	0.005	12.3	0.8	23.1	5.8

TABLE 1 - Stability of the phase control (at 6 σ) as measured with fluxes from 0.48 to 0.005 nW.

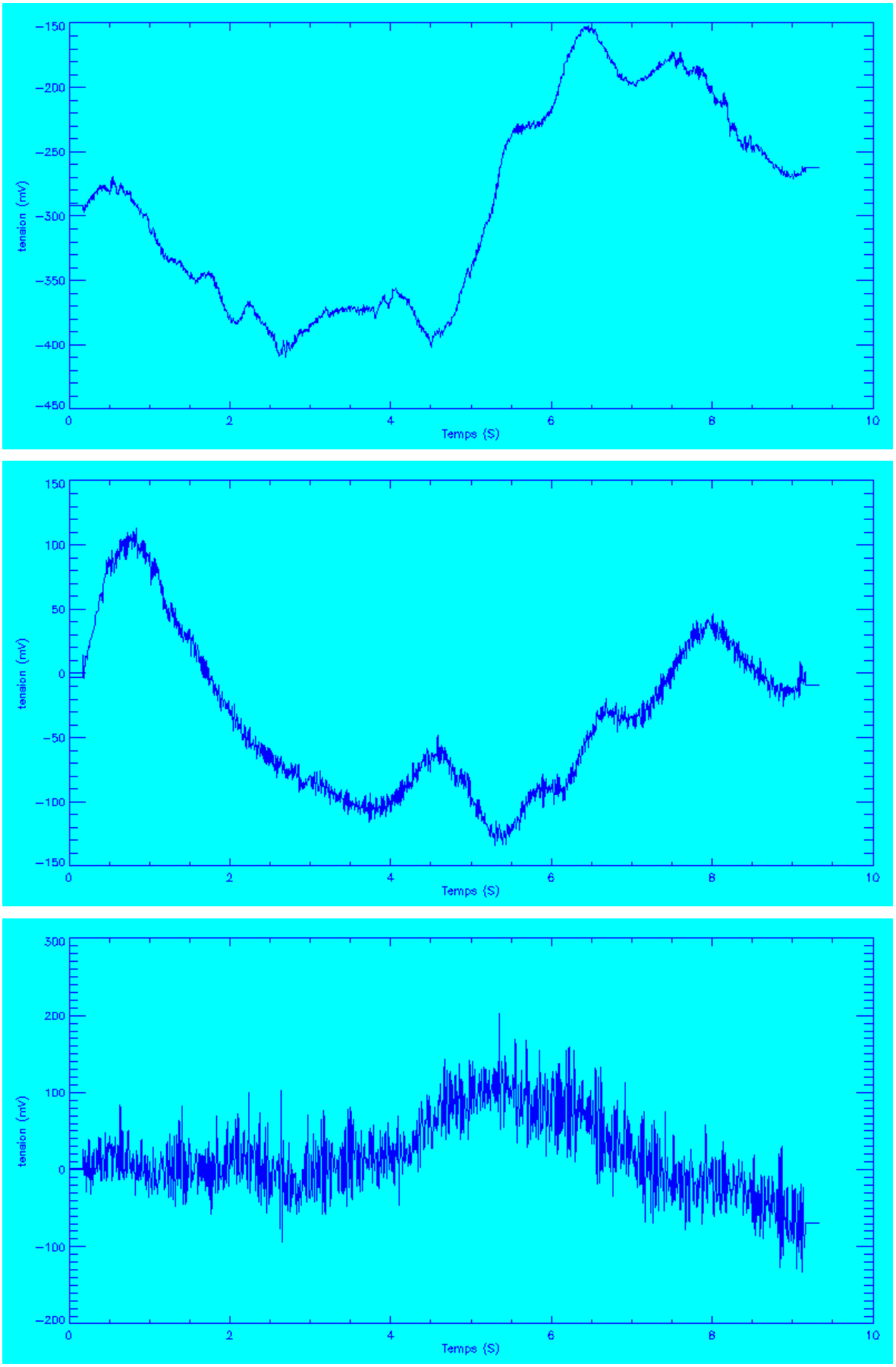

Fig. 7 - Examples of 10 seconds recording of the control signal obtained with the neutral density filters 0.3 (50% transmission), 0.6 (25%) and 1.6 (2.5%). These clearly show correction details up to 10 Hz but also some higher frequency noise, especially at low flux.

Magnitude (m_v)	Stability λ/ (pp @ **6**σ)
7.2	1083
8.0	620
8.7	447
9.8	152
10.5	46
11.3	31
12.3	17

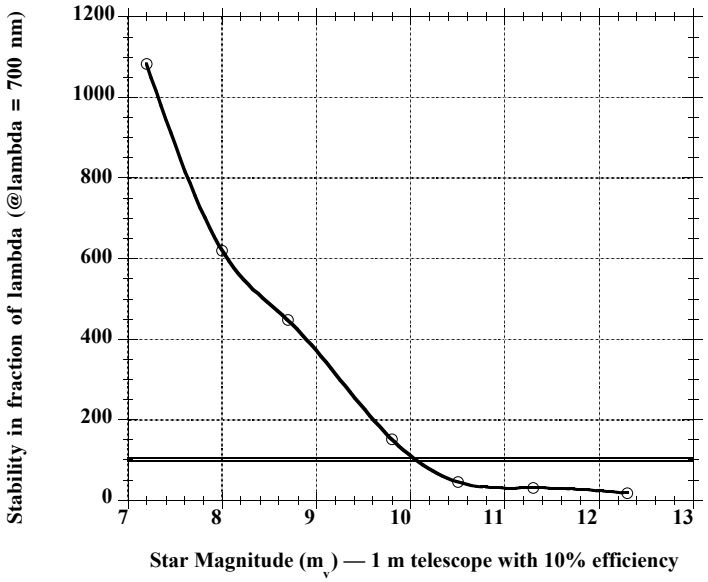

Fig. 8 - When corrected for the low contrast (28%) of the measurements due to the dispersion (as explained below) a more reasonable value of the stabilities to expect are (corrected only by a factor 3 compared to Table 1) definitively better than λ/100 for stars of magnitude 10 or more.

This correction of a factor 3 is very conservative since, beside the contrast, the dispersion also multiplies the number of fringes and, thus, lowers the chances to properly detect the correct amplitude for the central fringe. It is almost certain that, in good conditions an extra factor 2 (1 magnitude) could be gained. This would not be far from access to a reference star magnitude of 12 with λ/100 stability.

7 - INTERPRETATION OF THE OBSERVED ASYMMETRIES BY THE DISPERSION

Because of the beamsplitters, the thickness of glass can be slightly different in one arm of the interferometer than the other. This can be extremely annoying since the dispersion which is different between the blue and the red part of the large spectrum will be slightly affected. In practice if, like in our case, the global transmission (source, optics, detector) has the bad idea to have two peaks (cf. Fig. 9) then the errors on the glass balance in the two arms of the interferometer can affect both the maximum contrast and the position of the central fringe, as shown on Fig. 10. As can be noticed with 300 μm of unbalanced glass, we fairly well reproduce our signal and its contrast (about 30%). 300 μm is not so much since each % of variation on the beamsplitter (2.5 mm thick) will introduce 28 μm and since each degree of rotation of a beamsplitter will produce 13.7 μm (one of the equalization beamsplitter used was more than 10° misoriented - what we did not pay attention to before these simulations). Notice that this is really a spectral effect since the fringe spacing is smaller on the left (blue side) than the right (red side), as expected for the wavelength value.

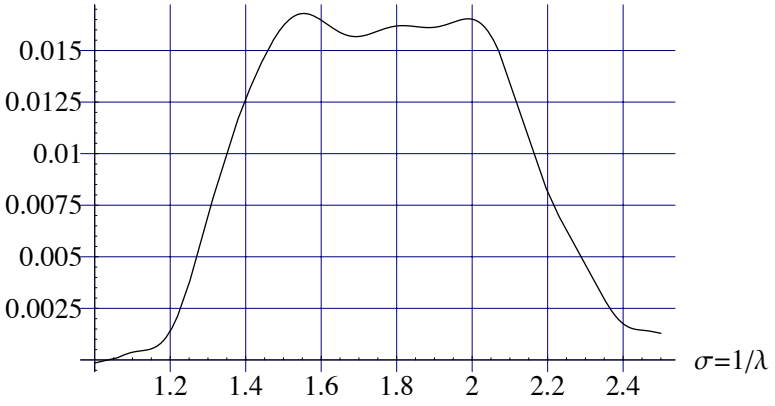

Fig. 9 - Global transmission of the source, optics and detector in the experiment. Notice that the source could nearly be considered as a triple "gaussian" source.

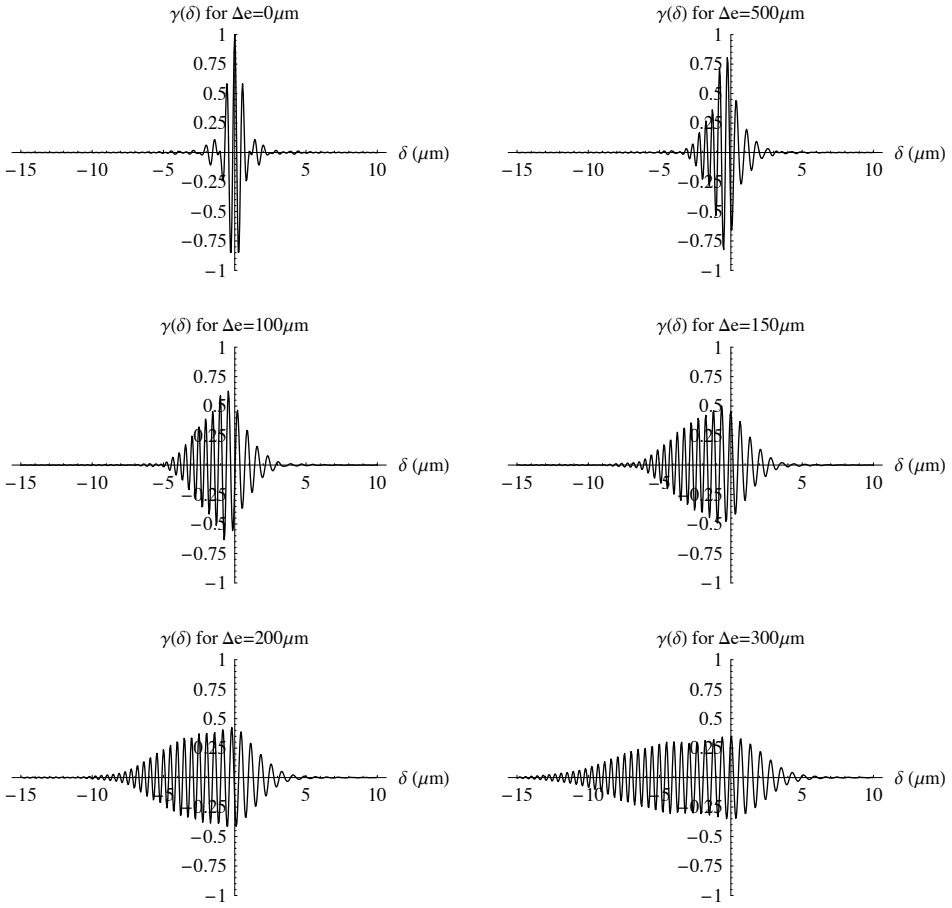

Fig. 10 - Coherence calculation accounting for a glass thickness in excess in one arm of the reference interferometer. Notice the lower contrast, larger number of fringes and shift of the fringes.

8- CONCLUSION

We have demonstrated without ambiguities that cophasing of two telescopes of 1 meter, assuming a transmission of 10% and using our method of double synchronous detection, can be achieved at $\lambda/100$ pp at $\mathbf{6}\sigma$ on (reference) stars as faint as magnitude 10 and, most probably, 12.

Another important result is that a large spectrum as the one used during these measurements has an evident advantage in term of flux and fringes identification but that its implementation in a working instrument will require a careful calibration of the reference interferometers in order to avoid path differences in glass which affect differentially the blue and red part of the spectrum.

Acknowledgments. We are particularly grateful to Michel Hersé who lend us the absolute photometer which made that study feasible and to CNES, ESA and MATRA MARCONI SPACE for providing financial support for this study

REFERENCES

[Alle 55] Allen, C.W.: 1955, "Astrophysical Quantities", The Athlone Press

[Dam 97] Damé, L.: 1997, "A Revolutionary Concept for High Resolution Solar Physics: Solar Interferometry", ESA Symposium on *Scientific Satellites Achievements and Prospects in Europe*, Paris, France, 20–22 November 1996, (to be published)

[Dam 97] Damé, L., Hersé, M., Kozlowski, M., Martic, M., Merdjane, M. and Moity, J.: 1997, Forum THEMIS — Science with THEMIS, Meudon, France, 14–15 November 1996, Eds. N. Mein and S. Sahal-Bréchot, Publication de l'Observatoire de Paris, 187

[Dam 96] Damé, L.: 1996, ESA Symp. on *Space Station Utilization*, Darmstadt, 30 Sept.–2 Oct. 1996, Ed. T.D. Guyenne, ESA SP-**385**, 369

[Dam 95] Damé, L., Derrien, M., Kozlowski, M. and Ruilier, C.: 1995, 27th JOSO Meeting, Benesov, Tcheque Republic, 12–15 November 1995, *JOSO Annual Report* **1995**, 52-59

[Dam 94] Damé, L.: 1994, "Solar Interferometry: Space and Ground Prospects", in *Amplitude and Intensity Spatial Interferometry II*, Ed. J.B. Breckinridge, Proc. SPIE–**2200**, 35–50